Transformation of the C_2H Ligand in $Fp^*C{\equiv}CH$ ($Fp^* = (\eta^5\text{-}C_5Me_5)Fe(CO)_2$) into Various C_2 Functional Groups via an Iron-Substituted Manganese Vinylidene Complex, $(\eta^5\text{-}C_5H_4Me)Mn(CO)_2[{=}C{=}C(H)Fp^*]$: Its Amphoteric Reactivities, Structural Comparisons Relevant to 1-Alkyne-to-Vinylidene Rearrangements, and Electronic Influences on Structures of Heterobimetallic Bridging Alkynyl Complexes $[(\eta^5\text{-}C_5R_5)M(CO)_2]_2(\mu\text{-}C_2R)$[1]

Munetaka Akita,* Naomi Ishii, Akio Takabuchi, Masako Tanaka, and Yoshihiko Moro-oka*

Research Laboratory of Resources Utilization, Tokyo Institute of Technology, 4259 Nagatsuta, Midori-ku, Yokohama 227, Japan

Received September 2, 1993®

The iron-substituted vinylidene complex $Cp'Mn(CO)_2[{=}C{=}C(H)Fp^*]$ (**4**) forms via a ligand replacement of $Cp'Mn(CO)_2(THF)$ with $Fp^*C{\equiv}CH$ (**3**) followed by a 1,2-H shift. **4** has been characterized as a hybrid of the η^1-vinylidene structure (**4B**, the dominant contributor) and the zwitterionic structure $[Cp'Mn^-(CO)_2C{\equiv}CH]Fp^{*+}$ (**4D**) in contrast to previously reported dinuclear bridging alkynyl complexes $M1M2(\mu\text{-}C_2R)$ which lie between the η^2-alkyne complex type structure $(\eta^2\text{-}M1C{\equiv}CR)M2$ (**A**) and the η^1-vinylidene structure $M1{=}C{=}C(R)M2$ (**B**). The C_2H ligand in **4** is transformed successfully to various elementary C_2 species via simple acid–base reactions. Deprotonation of **4** with *n*-BuLi generates an anionic ethynediyl intermediate, $Li[Cp'Mn(CO)_2C_2Fp^*]$ (**6**), and both of its bridging carbon atoms, on treatment with electrophiles, serve as a reaction site depending on their size. The reaction with H^+ (a small electrophile) is an orbital-controlled one to regenerate **4** through protonation at the slightly more negatively charged C_β (adjacent to Fe) with the larger HOMO coefficient, whereas the reaction at C_β with MeI (a bulky electrophile) is hindered by the sterically congested Cp* ligand to produce the η^2-alkyne complex $Cp'Mn(CO)_2(\eta^2\text{-}Fp^*C{\equiv}CMe)$ (**7**) through methylation at C_α (adjacent to Mn). On the other hand, **4** is readily protonated at C_β to give the cationic μ-vinylidene complex $[Cp'Mn(CO)_2Fp^*(\mu\text{-}C{=}CH_2)]$ ($\mathbf{8}^+$) via an Fe slippage. Reduction of $\mathbf{8}^+$ with NEt_4BH_4 affords the vinyl complex $Fp^*CH{=}CH_2$ (**9**) by way of hydride addition to the bridging carbon atom in $\mathbf{8}^+$. EHMO calculations on $M1M2(\mu\text{-}C_2R)$ (a hybrid of **A**, **B**, and **D**) including **4** and **7** reveal that its structure depends on a balance of π-eletron-donating abilities of M1 and M2. As one of the two metal centers becomes more electron donating and the other becomes less so, the structure changes from **A** to **B**. Related mono- and dinuclear complexes can be arranged according to the structural continuum **A**–**B** which is consistent with the electron-donating abilities of the metal centers. In addition, the MO characteristics observed for the structural change **A** → **B** are very similar to those of the intramolecular 1,2-H shift mechanism proposed for the 1-alkyne-to-vinylidene ligand rearrangement within a metal coordination sphere and thus the dinuclear complexes can be viewed as intermediate states of the 1,2-H shift.

Introduction

Coordination chemistry of the alkynyl (C_2R) ligand incorporated in a polymetallic system ($M_m(\mu_n\text{-}C_2R)$) has been studied extensively as a model for surface-bound hydrocarbyl species.[2] Previous studies on dinuclear complexes ($m = n = 2$)[3,4] have analyzed their structure as a resonances hybrid of three canonical structures, i.e. the metal-substituted η^2-alkyne complex type structure (**A**), the metal-substituted η^1-vinylidene structure (**B**), and the symmetrically bridging structure (**C**) (Chart 1). Because the third structure (**C**)[2,5] is quite rare, the structures of most dinuclear complexes $[M_2(\mu\text{-}C_2R)]$ lie between the two extremes **A** and **B** and are in fact closer to **A**. However, electronic factors determining their structures have not been elucidated so far. One of the reasons is that many of the examples contain a metal–metal bond and/or an additional bridging ancillary ligand such as dppm (1,2-bis(diphenylphosphino)methane) in A-frame complexes, which obscure intrinsic electronic interactions among the C_2R bridge and the two metal centers. Recently, a series of dinuclear complexes bearing $\mu\text{-}C_2R$ as a unique bridging ligand and 16e $(\eta^5\text{-}C_5R_5)ML_2$ species as metal components was reported by us[6] and others.[4]

In a previous paper[6a] we reported the structure and divergent fluxional behavior of the cationic diiron μ-acetylide complexes $[Fp^*_2(\mu\text{-}\eta^1{:}\eta^2\text{-}C{\equiv}CR)]BF_4$ (R = H (**1**), Ph

• Abstract published in *Advance ACS Abstracts*, December 1, 1993.

(1) Abbreviations: $Cp^* = \eta^5\text{-}C_5Me_5$; $Cp' = \eta^5\text{-}C_5H_4Me$; $Cp = \eta^5\text{-}C_5H_5$; $Fp^* = Cp^*Fe(CO)_2$; $Fp = CpFe(CO)_2$. Throughout this paper the carbon atoms of the C_2H and C_2 bridges bonded to Mn and Fe are designated as C_α and C_β, respectively.

(2) (a) Sappa, E.; Tiripicchio, A.; Braunstein, P. *Chem. Rev.* **1983**, *83*, 203–239. (b) Silvestre, J.; Hoffmann, R. *Langmuir* **1985**, *1*, 621–647. (c) Raithby, P. R.; Rosales, M. J. *Adv. Inorg. Chem. Radiochem.* **1985**, *29*, 169–247. (d) Nast, R. *Coord. Chem. Rev.* **1982**, *47*, 89–124.

0276-7333/94/2313-0258$04.50/0

Chart 1

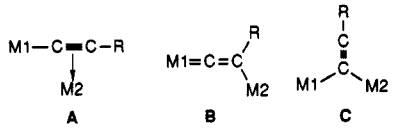

(2)), which were prepared from Fp*C≡CR and $[Fp^{*+}(THF)]BF_4^-$ (Scheme 1). In marked contrast to the fluxional behavior of the Ph derivative (2), which was explained readily by the conventional "windshield wiper"-like oscillation,[7] the mechanism for the μ-ethynyl complex (1) involved intramolecular 1,2-H migration. Since the spectroscopic and crystallographic characterization of 1 revealed the contribution of 1B in addition to the dominant A-type structure (1A and 1A'), the degenerate interconversion (1A → (1A' ↔) 1B) offered the first direct experimental evidence for the intramolecular 1,2-H shift mechanism which was proposed for the 1-alkyne-to-vinylidene rearrangement within a metal coordination sphere (eq 1).[8] Although this tautomerization has been

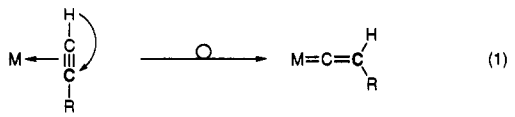

(1)

recognized as a key step in catalytic transformations of 1-alkynes,[9] this widely accepted mechanism had been supported so far only by the EHMO calculation by

Scheme 1

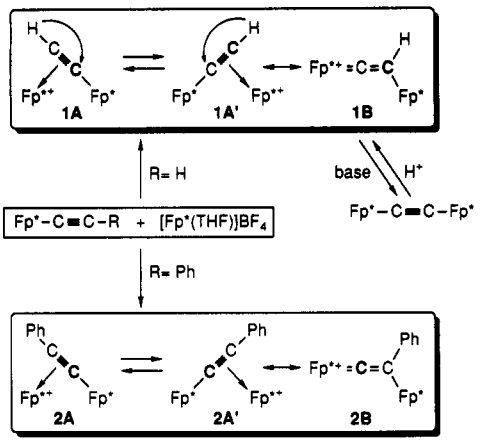

Hoffmann et al.[10] In addition, a closely related mechanism was postulated for interpretation of the ^{13}C CP/MAS NMR spectrum of acetylene adsorbed on a Pt/alumina catalyst.[11]

As an extension, we have investigated the interaction of Fp*C≡CH (3) with a $Cp'Mn(CO)_2$ species, which is isoelectronic with the Fp^{*+} species. Herein we report the structure and amphoteric reactivities of the resulting iron-substituted vinylidene complex $Cp'Mn(CO)_2[=C=C(H)-Fp^*]$ (4), the first example of a B-type complex. Furthermore, accumulated structural data for a series of $[(\eta^5-C_5R_5)M(CO)_2]_2(\mu-C_2R)$-type complexes enable us to elucidate the electronic effects of isoelectronic 16e $(\eta^5-C_5R_5)M(CO)_2$ fragments on the structures of the resulting dinuclear μ-alkynyl complexes.

Experimental Section

General Considerations. All manipulations were carried out under an argon atmosphere by using standard Schlenk tube techniques. Ether, THF, and hexanes (Na–K alloy) and CH_2Cl_2 (P_2O_5) were treated with appropriate drying agents, distilled, and stored under Ar. 3 was prepared according to the method described in our previous paper.[6a] $Cp'Mn(CO)_3$ (Alfa), *n*-BuLi (Aldrich), $HBF_4{\cdot}OEt_2$ (Aldrich), and NEt_4BH_4 (Tokyo Chemical Industry) were purchased and used as received. Column chromatography and preparative TLC were performed on alumina (column, activity II–IV (Merck Art. 1097); PTLC, aluminum oxide 60 PF_{254} (Type E) (Merck Art. 1103)).

^1H and ^{13}C NMR spectra were recorded on JEOL EX-90 (^1H, 90 MHz) and JEOL GX-270 spectrometers (^1H, 270 MHz; ^{13}C, 67.9 MHz). Solvents for NMR measurements containing 1% TMS were dried over molecular sieves and distilled under reduced pressure. IR and FD-MS spectra were obtained on a JASCO FT/IR 5300 spectrometer and a Hitachi M-80 mass spectrometer, respectively.

Preparation of 4. A THF solution (500 mL) of $Cp'Mn(CO)_3$ (1.58 mL, 10 mmol) in a Pyrex photoreactor immersed in an ice–water bath was irradiated by a high-pressure mercury lamp for 8 h with a slow argon purge. After conversion of $Cp'Mn(CO)_3$ (2001, 1916 cm^{-1}) to $Cp'Mn(CO)_2(THF)$ (1921, 1839 cm^{-1}) was confirmed by IR, 3 (1.905 g, 7.00 mmol) was added to the resulting solution, and the mixture was stirred for 17 h at ambient

(3) (a) Carty, A. J. *Pure Appl. Chem.* **1982**, *54*, 113–130. (b) Cherkas, A. A.; Randall, L. H.; MacLaughlin, S. A.; Mott, G. M.; Carty, A. J. *Organometallics* **1988**, *7*, 969–977. (c) Abu Salah, O. M.; Bruce, M. I. *J. Chem. Soc., Dalton Trans.* **1974**, 2302–2304, 2311–2315. (d) Ciriano, M.; Howard, J. A. K.; Spencer, J. L.; Stone, F. G. A.; Wadepohl, H. *J. Chem. Soc., Dalton Trans.* **1979**, 1749–1756. (e) Hutton, A. T.; Shebanzadeh, B.; Shaw, B. L. *J. Chem. Soc., Chem. Commun.* **1984**, 549–551. (f) Hutton, A. T.; Langrick, C. R.; McEwan, D. M.; Pringle, P. G.; Shaw, B. L. *J. Chem. Soc., Dalton Trans.* **1985**, 2121–2130. (g) Nubel, P. O.; Brown, T. L. *Organometallics* **1984**, *3*, 29–32. (h) Deranyagala, S. P.; Grundy, K. R. *Organometallics* **1985**, *4*, 424–426. (i) Cowie, M.; Loeb, S. J. *Organometallics* **1985**, *4*, 852–857. (j) Carriedo, G. A.; Miguel, D.; Riera, V.; Solans, X.; Font-Altaba, M.; Coll, M. *J. Organomet. Chem.* **1986**, *299*, C43–46. (k) Erker, G.; Fromberg, W.; Benn, R.; Mynott, R.; Angermund, K.; Kruger, C. *Organometallics* **1989**, *8*, 911–920. (l) Seyferth, D.; Hoke, J. B.; Wheeler, D. R. *J. Organomet. Chem.* **1988**, *341*, 421–437. (m) Fritz, P. M.; Polborn, K.; Steimann, M.; Beck, W. *Chem. Ber.* **1989**, *122*, 889–891. (n) Koridze, A. A.; Kizas, O. A.; Petroviskii, P. V.; Kolobova, N. E.; Struchkov, Y. T.; Yanovsky, A. I. *J. Organomet. Chem.* **1988**, *338*, 81–87. (o) Fornies, J.; Gomez-Saso, M. A.; Martinez, F.; Moreno, M. T. *Organometallics* **1992**, *11*, 2873–2883. (p) Esteruelas, M. A.; Lahuerta, O.; Modrego, J.; Nurnberg, O.; Oro, L. A.; Rodríguez, L.; Sola, E.; Werner, H. *Organometallics* **1993**, *12*, 266–275

(4) (a) Kolobova, N. E.; Skripkin, V. V.; Rozantseva, T. V.; Struchkov, Y. T.; Aleksandrov, G. G.; Andrianov, V. G. *J. Organomet. Chem.* **1981**, *218*, 351–359. (b) Appel, M.; Heidrich, J.; Beck, W. *Chem. Ber.* **1987**, *120*, 1087–1089. (c) Frank, K. G.; Selegue, J. P. *J. Am. Chem. Soc.* **1990**, *112*, 6414–6416.

(5) The C-type structure is found frequently in the complexes of Cu and main-group elements. See for example: (a) van Koten, G. *J. Organomet. Chem.* **1990**, *400*, 283–301. (b) ten Hoedt, R. W. M.; Noltes, J. G.; van Koten, G.; Speck, A. L. *J. Chem. Soc., Dalton Trans.* **1978**, 1800–1806. (c) van Koten, G.; ten Hoedt, R. W. M.; Noltes, J. G. *J. Org. Chem.* **1977**, *42*, 2705–2711. (d) Carty, A. J.; Taylor, N. J.; Smith, W. F. *J. Chem. Soc., Chem. Commun.* **1979**, 750–751. (e) Morosin, B.; Howatson, J. *J. Organomet. Chem.* **1971**, *29*, 7–14. (f) Reference 3e.

(6) (a) Akita, M.; Terada, M.; Oyama, S.; Moro-oka, Y. *Organometallics* **1990**, *9*, 816–825. (b) Akita, M.; Terada, M.; Oyama, S.; Sugimoto, S.; Moro-oka, Y. *Organometallics* **1991**, *10*, 1561–1568. (c) Akita, M.; Terada, M.; Moro-oka, Y. *Organometallics* **1991**, *10*, 2962–2965. See also: (d) Akita, M.; Terada, M.; Moro-oka, Y. *Organometallics* **1992**, *11*, 1825–1830. (e) Akita, M.; Terada, M.; Moro-oka, Y. *Organometallics* **1992**, *11*, 3468–3472. (f) Akita, M.; Sugimoto, S.; Tanaka, M.; Moro-oka, Y. *J. Am. Chem. Soc.* **1992**, *114*, 7581–7582.

(7) See, for example, refs 3 and 6a. See also: Hwang, D.-K.; Chi, Y.; Peng, S.-M.; Lee, G.-H. *Organometallics* **1990**, *9*, 2709–2718.

(8) (a) Bruce, M. I. *Chem. Rev.* **1991**, *91*, 197–257. (b) Bruce, M. I.; Swincer, A. G. *Adv. Organomet. Chem.* **1983**, *22*, 60–128.

(9) (a) Wakatsuki, Y.; Yamazaki, H.; Kumegawa, N.; Satoh, T.; Satoh, J. Y. *J. Am. Chem. Soc.* **1991**, *113*, 9604–9610. (b) Trost, B. M.; Kulawiec, R. J. *J. Am. Chem. Soc.* **1992**, *114*, 5579–5584. (c) References cited in ref 8a.

(10) Silvestre, J.; Hoffmann, R. *Helv. Chim. Acta* **1985**, *68*, 1461–1506.

(11) Chin, Y. H.; Ellis, P. D. *J. Am. Chem. Soc.* **1989**, *111*, 7653–7654. However, Haw et al. very recently claimed that the ^{13}C NMR signal was due to an adsorbed benzene species resulting from cyclotrimerization of acetylene: Lambregts, M. J.; Munson, E. J.; Kheir, A. A.; Haw, J. J. *J. Am. Chem. Soc.* **1992**, *114*, 6875–6879.

temperature. Then the volatiles were removed under reduced pressure, and products were extracted with ether and separated by column chromatography (3 cm × 20 cm). Cp'Mn(CO)$_3$ and Fp*$_2$ were eluted with ether–hexanes (1:20). Then a brown band eluted with ether–hexanes (1:10) was collected, from which **4** (1.21 g, 2.6 mmol, 37% yield) was isolated as brown crystals after crystallization from ether–hexanes. **4**: ^{1}H NMR (C_6D_6) δ 1.41 (15 H, s, Cp*), 1.85 (3H, s, C_5H_4Me), 4.46 (4H, m, C_5H_4Me), 4.62 (1H, s, μ-C_2H); ^{13}C NMR (C_6D_6) δ 9.5 (q, $^1J_{CH}$ = 128.7 Hz, C_5Me_5), 13.8 (q, $^1J_{CH}$ = 128.7 Hz, C_5H_4Me), 84.8 (d, $^1J_{CH}$ = 176.5 Hz, C_5H_4Me), 85.9 (d, $^1J_{CH}$ = 176.5 Hz, C_5H_4Me), 91.2 (d, $^1J_{CH}$ = 171.0 Hz, =CH), 96.1 (s, C_5Me_5), 104.8 (s, *C*Me in Cp'), 217.8 (Fe—CO), 232.3 (Mn—CO), 310.5 (s, Mn=C); IR (KBr) ν(C≡O) 1991, 1955, 1945, 1885, ν(C=C) 1641 cm^{-1}; FDMS *m/z* 462 (M$^+$). Anal. Calcd for $C_{22}H_{23}O_4FeMn$: C, 57.17; H, 5.02. Found: C, 57.13; H, 5.19.

Deuteration of 4 by the Action of Base. *n*-BuLi. To a THF solution (3 mL) of **4** (46 mg, 0.10 mmol) cooled at −78 °C was added *n*-BuLi (1.55 M hexane solution, 0.07 mL, 0.11 mmol). The mixture was stirred for 70 min at the same temperature, and then EtOD (0.1 mL, 1.7 mmol) was added. After the mixture was warmed to room temperature, the volatiles were removed under reduced pressure, and the product was extracted with ether and filtered through an alumina pad. The ^{1}H NMR spectrum of the residue obtained by evaporation of the filtrate showed the quantitative formation of **4-*d***, as indicated by the disappearance of C_2H. ν(C=C): 1623 cm^{-1}. FDMS: 463 (M$^+$).

NaOEt. To **4** (46 mg, 0.10 mmol) dissolved in THF (3 mL) was added a EtONa–EtOD solution (0.87 M, 1.4 mL, 0.10 mmol), and the mixture was stirred for 2 h at ambient temperature. After evaporation of the volatiles the residue was worked up as described above. The quantitative deuteration was confirmed by ^{1}H NMR and IR. Prolonged reaction afforded Fp*$_2$. In the absence of NaOEt deuteration was not observed at all.

Preparation of 7. A THF solution (9 mL) of **6** was generated from **4** (139 mg, 0.301 mmol) and *n*-BuLi (1.54 M hexane solution, 0.33 mL, 0.56 mmol) at −78 °C as described above. To the resulting solution was added MeI (0.18 mL, 2.8 mmol) dropwise. The mixture was warmed gradually and stirred at room temperature for 30 min. After removal of the volatiles under reduced pressure the product was extracted with ether and filtered through an alumina pad. Crystallization from ether–hexanes gave **7** (64 mg, 0.13 mmol, 46% yield) as orange crystals. **7**: ^{1}H NMR (C_6D_6) δ 1.47 (15H, s, Cp*), 1.73 (3H, s, C_5H_4Me), 2.56 (3H, s, *Me*C≡), 4.3 (4H, br, C_5H_4Me); ^{13}C NMR (C_6D_6) δ 9.6 (q, $^1J_{CH}$ = 127 Hz, C_5Me_5), 13.2 (q, $^1J_{CH}$ = 128 Hz, C_5H_4Me), 15.8 (q, $^1J_{CH}$ = 127 Hz, *Me*C≡), 67.8, 73.3 (s × 2, C≡C), 82.0 (d, J = 172 Hz, C_5H_4Me), 84.3 (d, $^1J_{CH}$ = 175 Hz, C_5H_4Me), 97.2 (s, C_5Me_5), 103.2 (s, *C*Me in Cp'), 216.6 (s, Fe—CO), 225.8 (s, Mn—CO); IR (KBr) ν(C≡O) 1998, 1963, 1917, ν(C≡C) 1839 cm^{-1}; FDMS *m/z* 476 (M$^+$). Anal. Calcd for $C_{23}H_{25}O_4FeMn$: C, 58.01; H, 5.29. Found: C, 58.07; H, 5.22.

Protonation of 4. To a CH_2Cl_2 solution (50 mL) of **4** (92 mg, 0.20 mmol) was added HBF_4·OEt_2 (0.22 M CH_2Cl_2 solution, 0.92 mL, 0.20 mmol) via a syringe. The solution immediately turned red. After the mixture was stirred at room temperature for 5 min, the volatiles were removed under reduced pressure. Products were extracted with CH_2Cl_2 and filtered through a Celite pad. Addition of ether afforded a red-purple powder (**8**-BF_4: 79 mg, 0.14 mmol, 70% yield). An analytically pure sample was not obtained. ^{1}H NMR ($CDCl_3$): δ 1.89 (15H, s, C_5Me_5), 2.10 (3H, s, C_5H_4Me), 4.71, 4.86, 4.92, 5.08 (1H × 4, br s, C_5H_4Me), 6.78, 7.14 (1H × 2, d, J = 11.5 Hz, =CH_2). ^{13}C NMR ($CDCl_3$): δ 9.8 (q, J = 131 Hz, C_5Me_5), 9.9 (q, J = 131 Hz, C_5H_4Me), 88.5, 91.5, 93.5, 93.8 (d × 4, J not analyzed, C_5H_4Me), 104.1 (s, C_5Me_5), 104.8 (s, ipso-C in Cp'), 132.8 (t, J = 160 Hz, CH_2), 205.0, 209.0 (s × 2, Fe—CO), 227.0, 228.7 (s × 2, Mn—CO), 280.1 (s, C=CH_2). IR (CH_2Cl_2): ν(C≡O) 2051, 2013, 1996, 1975 cm^{-1}. FD-MS: *m/z* 463 (8$^+$). On protonation of **4** with CF_3SO_3H and CF_3COOH, IR spectra (2200–1500 cm^{-1}) identical with that of **8**-BF_4 except for the CF_3COO absorptions were obtained.

Acid-Catalyzed H–D Exchange of 4. With a Catalytic Amount of CF_3COOH. To a CH_2Cl_2 solution (3 mL) of **4** (56 mg, 0.12 mmol) was added EtOD (0.5 mL) and CF_3COOH (1 μL, 0.012 mmol, 10 mol %). The resulting mixture was stirred for 30 min at room temperature. An IR spectrum showed quantitative formation of **4-*d***. Evaporation of the volatiles, extraction with ether, filtration through an alumina pad, and removal of the solvent gave **4-*d*** (50 mg, 89%).

With an Excess Amount of CH_3COOH. To a CH_2Cl_2 solution (2 mL) of **4-*d*** (50 mg, 0.108 mmol) was added CH_3COOH (0.54 mmol, 30 μL). Spontaneous formation of **4** was confirmed by IR. Removal of CH_3COOH by addition of Et_3N (0.1 mL, 0.72 mmol) followed by the workup as described above gave **4** (46 mg, 92%).

Conversion of 4 to Fp*CH=CH_2 (9). To a CH_2Cl_2 solution (2 mL) of **4** (46 mg, 0.10 mmol) was added HBF_4·OEt_2 (20 μL, 0.14 mmol) at ambient temperature. The protonation took place at once, as judged by IR. Then, an excess of NEt_4BH_4 was added to the mixture. After this mixture was stirred for 10 min at room temperature, the volatiles were removed under reduced pressure. Extraction with ether and filtration through an alumina pad followed by separation by preparative TLC gave a yellow oil, whose spectral data (^{1}H and ^{13}C NMR and IR) were identical with those of an authentic sample of Fp*CH=CH_2 (**9**).[12] Because we could not get a pure sample, the yield was determined by ^{1}H NMR using dimethyl terephthalate as an internal standard. In the deuteration experiment, CF_3COOD was used in place of HBF_4·OEt_2.

X-ray Crystallography of 4 and 7. **4** and **7** were recrystallized from an ether–hexanes mixed solvent system, and suitable crystals were mounted on glass fibers. Diffraction measurements were made on a Rigaku AFC-5R automated four-circle diffractometer by using graphite-monochromated Mo Kα radiation (λ = 0.710 59 Å). The unit cell was determined and refined by a least-squares method using 24 independent reflections. Data were collected with an ω–2θ scan technique. If $\sigma(F)/F$ was more than 0.1, a scan was repeated up to three times and the results were added to the first scan. Three standard reflections were monitored every 150 measurements. All data processing was performed on a Micro Vax II computer by using the TEXSAN structure-solving program system obtained from the Rigaku Corp., Tokyo, Japan. Neutral scattering factors were obtained from the standard source.[13] In the reduction of data, Lorentz, polarization, and empirical absorption corrections (ψ scan) were made.

The structures were solved by a combination of direct methods and Fourier synthesis (MITHRIL and DIRDIF). All the nonhydrogen atoms were refined anisotropically. All the hydrogen atoms except H1 of **4** were fixed at the calculated positions (C–H = 0.95 Å) and were not refined. H1 of **4** was refined isotropically. The crystallographic data and positional and selected structural parameters of **4** and **7** are summarized in Tables 1–3. For the core structures, see also Figure 2 and Table 6.

EHMO Calculations of 4 and 6. The EHMO parameters were taken from ref 9. The structures of the CpM(CO)$_2$ fragments were approximated by the following parameters irrespective of M (Fe, Mn): M–cp(the centroid of Cp), 1.73 Å; cp—C(Cp), 1.20 Å; C(Cp)—H(Cp), 1.00 Å; M—CO, 1.75 Å; C≡O, 1.15 Å; ∠cp—M—CO(X), 110°; dihedral angles defined by cp—M—CO and cp—M—X planes, 120°. For the bridging parts, the bond angles and bond lengths obtained from the crystallographic results were used. **4**: Mn—C_α, 1.84 Å; C_α—C_β, 1.27 Å; Fe—C_β, 2.04 Å. For **6**, the linear structure which was found for the isoelectronic

(12) An authentic sample of **9** (yellow waxy solid) was prepared by the reaction of Fp*I with CH_2=CH—MgBr in THF. ^{1}H NMR ($CDCl_3$): δ 1.76 (s, 15H, Cp*), 5.33 (1H, dd, J = 1.6 and 17.4 Hz, CH_2 *cis* to Fe), 5.88 (1H, dd, J = 1.5 and 9.2 Hz, CH_2 *trans* to Fe), 6.90 (1H, dd, J = 9.2 and 17.4 Hz). ^{13}C NMR ($CDCl_3$): δ 9.5 (q, J = 127.7 Hz, C_5Me_5), 95.7 (s, C_5Me_5), 126.7 (t, J = 151.9 Hz, CH_2), 155.0 (d, J = 142.5 Hz, CH), 217.5 (s, CO). IR (CH_2Cl_2): 1996, 1938 cm^{-1}.

(13) *International Tables for X-Ray Crystallography*; Kynoch Press: Birmingham, U.K., 1975; Vol. 4.

Table 1. Crystallographic Data for 4 and 7

	4	7
formula	$C_{22}H_{23}O_4FeMn$	$C_{23}H_{25}O_4FeMn$
fw	462.2	476.2
space group	$P\bar{1}$	$P2_1/n$
a, Å	10.680(6)	10.324(3)
b/Å	11.968(9)	13.062(2)
c/Å	8.792(5)	16.385(2)
α/deg	91.76(6)	
β/deg	110.60(4)	97.68(1)
γ/deg	87.38(5)	
V/Å³	1051(1)	2189.6(7)
Z	2	4
d_{calcd}/g cm^{-3}	1.461	1.445
μ/cm^{-1}	12.90	12.40
temp/°C	25	25
2θ/deg	5–50	5–50
no. of data collected	3927	4283
no. of data with $F^2 > 3\sigma(F^2)$	2717	2816
no. of variables	257	262
R	0.0624	0.0395
R_w	0.0730	0.0520

Table 2. Positional Parameters and B_{eq} Values (Å²) for 4

atom	x/a	y/b	z/c	B_{eq}
Fe	−0.15066(8)	0.23487(7)	0.2345(1)	3.46(4)
Mn	0.28626(9)	0.28448(8)	0.4468(1)	4.26(4)
O3	−0.2131(6)	0.1658(5)	0.5123(6)	7.4(3)
O4	0.0347(5)	0.0488(5)	0.2452(7)	6.4(3)
O5	0.2328(6)	0.2254(6)	0.1044(7)	7.8(3)
O6	0.3240(6)	0.5123(5)	0.3672(7)	8.0(3)
C1	−0.0146(6)	0.3414(6)	0.3819(8)	4.4(3)
C2	0.1086(6)	0.3196(5)	0.4083(7)	4.0(3)
C3	−0.1847(6)	0.1934(6)	0.4061(8)	4.6(3)
C4	−0.0346(7)	0.1266(6)	0.2448(7)	4.4(3)
C5	0.2529(6)	0.2488(6)	0.239(1)	5.2(3)
C6	0.3109(7)	0.4224(7)	0.4015(8)	5.3(3)
C10	−0.3500(6)	0.2199(5)	0.0797(7)	3.9(2)
C11	−0.2654(6)	0.1880(6)	−0.0050(7)	4.3(3)
C12	−0.1873(6)	0.2815(6)	−0.0078(7)	4.5(3)
C13	−0.2294(6)	0.3721(5)	0.0730(8)	4.4(3)
C14	−0.3288(6)	0.3329(5)	0.1301(7)	4.1(3)
C15	−0.4524(7)	0.1477(7)	0.1058(9)	5.9(3)
C16	−0.2626(8)	0.0772(7)	−0.0885(8)	6.3(4)
C17	−0.0908(8)	0.2880(8)	−0.097(1)	7.4(4)
C18	−0.182(1)	0.4881(7)	0.086(1)	7.5(4)
C19	−0.4035(8)	0.4025(7)	0.216(1)	6.6(4)
C20	0.2939(7)	0.1785(6)	0.6463(8)	4.8(3)
C21	0.371(1)	0.2703(7)	0.7077(9)	6.7(4)
C22	0.474(1)	0.269(1)	0.643(1)	8.9(5)
C23	0.460(1)	0.178(1)	0.543(1)	8.3(5)
C24	0.3460(8)	0.1193(6)	0.5416(9)	5.8(3)
C25	0.177(1)	0.1435(9)	0.690(1)	8.6(5)
H1	−0.053(6)	0.403(5)	0.431(7)	5(1)

diiron complex Fp*C≡CFp* was assumed: M—C, 1.93 Å; C—C, 1.20 Å.[6b,14] An EHMO calculation program was obtained from ref 15.

Results

Preparation and Characterization of an Iron-Substituted Vinylidene Complex, Cp'Mn(CO)₂[=C=C(H)Fp*] (4). Treatment of the ethynyliron complex **3** with an *in situ* generated labile Mn species, $Cp'Mn(CO)_2(THF)$,[8,16,17] gave brown crystals of **4** in a moderate yield after chromatographic separation followed by crystallization from ether–hexanes (eq 2). **4** was characterized readily as an η^1-vinylidene complex on the basis of the diagnostic, highly deshielded quaternary carbon signal assignable to C_α[8] (δ 310.5 (Table 4)) and the strong ν(C=C) absorption (1641 cm^{-1}). However, the significant upfield shift of the C_2H ^{13}C signals from those of normal η^1-vinylidene Mn complexes ($\Delta\delta$(C1) = 31.1, $\Delta\delta$(C2) = 76.6 compared to $Cp'Mn(CO)_2(=C=CMe_2)$ (**5**)[18] (Table 4)) suggested that the introduction of the Fp* group as a vinylidene substituent might cause deformation; therefore, the molecular structure was determined by X-ray crystallography. A perspective view of **4** is reproduced in Figure 1 (see also Figure 2 and Tables 5 and 6). The bond angles associated with the bridging MnFe(μ-C_2H) part

Table 3. Positional Parameters and B_{eq} Values (Å²) for 7

atom	x/a	y/b	z/c	B_{eq}
Fe	0.92586(5)	0.27028(4)	0.33014(3)	2.83(2)
Mn	0.62119(6)	0.22111(5)	0.44400(4)	3.80(3)
O3	0.8102(3)	0.4688(3)	0.3547(2)	6.1(2)
O4	0.8020(4)	0.2383(3)	0.1627(2)	6.7(2)
O5	0.8150(4)	0.3439(3)	0.5475(2)	6.1(2)
O6	0.6534(4)	0.0627(3)	0.5700(2)	6.8(2)
C0	0.6766(5)	0.0063(4)	0.3585(3)	5.4(2)
C1	0.7855(4)	0.1893(3)	0.3672(2)	3.2(2)
C2	0.7185(4)	0.1135(3)	0.3743(2)	3.6(2)
C3	0.8534(4)	0.3901(3)	0.3454(2)	3.9(2)
C4	0.8493(4)	0.2520(3)	0.2287(3)	4.0(2)
C5	0.7418(5)	0.2943(3)	0.5051(3)	4.3(2)
C6	0.6413(4)	0.1253(4)	0.5194(3)	4.4(2)
C10	1.0625(4)	0.2021(3)	0.4237(2)	3.1(2)
C11	1.0949(4)	0.3058(3)	0.4148(2)	3.3(2)
C12	1.1203(4)	0.3217(3)	0.3324(3)	3.6(2)
C13	1.1045(4)	0.2271(3)	0.2910(2)	3.8(2)
C14	1.0657(4)	0.1525(3)	0.3464(2)	3.5(2)
C15	1.0377(4)	0.1508(4)	0.5014(3)	4.6(2)
C16	1.1135(4)	0.3836(3)	0.4820(3)	4.7(2)
C17	1.1666(4)	0.4197(4)	0.2985(3)	5.5(2)
C18	1.1319(5)	0.2049(4)	0.2057(3)	5.9(3)
C19	1.0453(5)	0.0409(3)	0.3297(3)	5.2(2)
C20	0.4889(5)	0.2637(6)	0.3329(4)	6.7(3)
C21	0.4284(5)	0.1899(5)	0.3787(4)	6.7(3)
C22	0.4194(6)	0.2347(7)	0.4557(5)	8.6(4)
C23	0.4743(8)	0.3310(8)	0.4583(5)	9.7(5)
C24	0.5156(6)	0.3485(5)	0.3841(6)	8.1(4)
C25	0.5126(7)	0.2545(7)	0.2469(4)	11.0(5)

Table 4. Comparison of ^{13}C NMR Data for 4 and 7 with Those for Related Complexes[a]

complex	δ(C1)	δ(C2)	δ(C2) − δ(C1)
10	66.7	75.4	8.7
11	44.3	46.2	1.9
7	67.8	73.3	5.5
2	85.7	109.3	23.6
1	72.2	124.2	52.0
12	142.5	198.6	56.1
5	122.3	387.1	264.8
4	91.2	310.5	219.3

[a] For the carbon atom numbering and the structures of the complexes, see Table 6 and Chart 2.

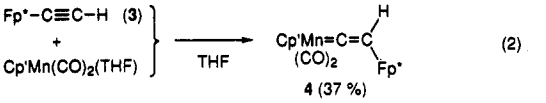

(2)

(14) A linear structure with a *trans* configuration such as Fp*C≡CFp* is assumed. Important bond lengths (Å) and angles (deg) for Fp*C≡CFp* (Fe1C1≡C2Fe2): Fe1–C1, 1.936(4); C1–C2, 1.209(4); C2–Fe2, 1.932(3); ∠Fe1–C1–C2, 172.7(3); ∠C1–C2–Fe2, 173.9(3). Akita, M.; Sugimoto, S.; Moro-oka, Y. To be submitted for publication.

(15) Nishimoto, K.; Imamura, A.; Yamaguchi, K.; Yamabe, S.; Kitaura, K. *Bunshisekkei-no-tame-no-ryoshikagaku (Quantum Chemistry for Molecular Design)*; Kodansha: Tokyo, 1989.

(16) (a) Strohmeier, W.; Hellmann, H. *Chem. Ber.* **1965**, *98*, 1598–1607. (b) Nesmyanov, A. N.; Aleksandrov, G. G.; Antonova, A. B.; Anisimov, K. N.; Kolobova, N. E.; Struchkov, Y. T. *J. Organomet. Chem.* **1976**, *110*, C36–38. (c) Antonova, A. B.; Kolobova, N. E.; Petrovsky, P. V.; Lokshin, B. V.; Obezyuk, N. S. *J. Organomet. Chem.* **1977**, *137*, 55–67.

(17) Caulton, K. G. *Coord. Chem. Rev.* **1981**, *38*, 1–43.

(18) Berke, H.; Huttner, G.; von Seyerl, J. *J. Organomet. Chem.* **1981**, *218*, 193–200.

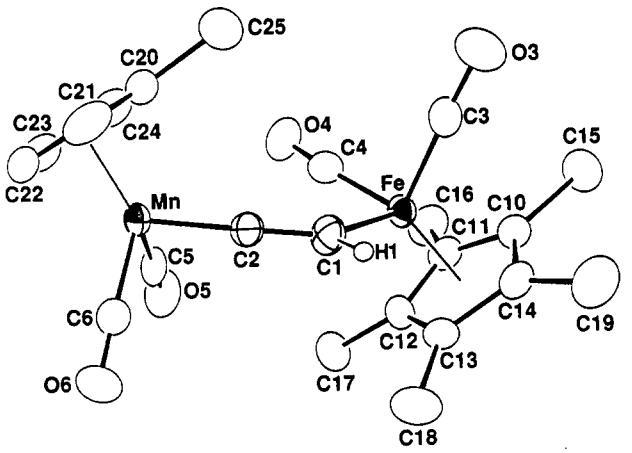

Figure 1. Perspective view of **4** drawn at the 30% probability level.

(∠Mn—C2—C1 (α) = 178.7(5)°, ∠C2—C1—Fe (γ) = 118.1(5)°) and no apparent interaction between Fe and C2 (d = 2.866(6) Å) indicate that **4** is viewed as an Fp*-substituted η^1-vinylidene Mn complex. However, (i) the Mn—C2 distance (a) of **4** is 0.05 Å longer and (ii) the C1—C2 distance (b) is 0.06 Å shorter than the corresponding bond lengths of **5**[18] (Table 6).

4 of the **B**-type structure results from a 1,2-H shift of the Fp*C≡CH ligand following eq 1, which is very common for the reactions of 1-alkynes with $(\eta^5\text{-}C_5R_5)Mn(CO)_2$ species.[8,16,17] It should be noted that the structure of **4** contrasts strikingly with that of **1** with the **A**-type dominant resonance structure (Figure 2), although both complexes are derived from **3** upon treatment with isoelectronic 16e $(\eta^5\text{-}C_5R_5)M(CO)_2$ species (M = Mn, Fe^+).

Deprotonation of 4 and Reactivity of the Resulting Anionic Species. The prototropic fluxional behavior of **1** and its deprotonation reaction producing Fp*C≡CFp* (Scheme 1)[6a,b,14] suggested a similar Brønsted acidic nature of **4**. As expected, treatment of **4** with an EtOD solution of NaOEt gave **4**-d (eq 3), and the deuteration was

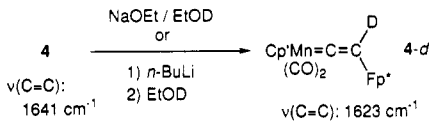

(3)

monitored readily by the red shift of ν(C≡C) by ca. 20 cm^{-1}. However, an intramolecular hydrogen shift as observed for **1** (Scheme 1)[6a] was not detected by ^1H NMR. The $\delta_H(C_2H)$ value did not change in the temperature range of −80 to +50 °C in toluene-d_8, and above 50 °C **4** decomposed gradually to give $Cp'Mn(CO)_3$ and Fp^*_2.

Irreversible deprotonation was effected by the action of n-BuLi. Treatment of a THF solution of **4** with n-BuLi at −78 °C generated an anionic species, Li[Cp'Mn(CO)$_2$C$_2$-Fp*] (**6**).[19] Addition of EtOD at the same temperature resulted in deuteration at the carbon atom adjacent to Fe (C_β)[1] to afford **4**-d (eq 3). In contrast to this regiochemistry, quenching with MeI resulted in methylation at the carbon atom adjacent to Mn (C_α)[1] in **6** to give the **A**-type product $Cp'Mn(CO)_2(\eta^2\text{-Fp*C≡CMe})$ (**7**), and a methyl-substituted vinylidene complex (a **B**-type product) was not

(19) Reaction of **4** with excess BuLi followed by quenching with electrophiles gave the μ-3-oxohept-1-en-1-yl complexes Cp'MnCp*Fe-[μ-CH=C(E)-C(=O)-Bu](μ-CO) (E = H, Me), resulting from a nucleophilic addition of the Bu group to a CO ligand: Akita, M.; Takabuchi, A.; Tanaka, M.; Moro-oka, Y. Unpublished results.

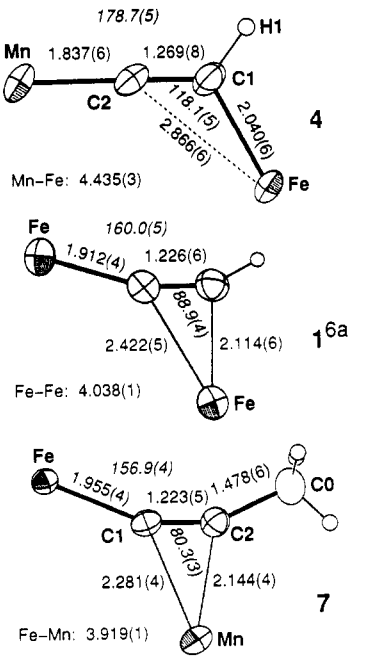

Figure 2. Structures of the bridging parts of **1**, **4**, and **7** (italic type, angles (deg); Roman type, lengths (Å)).

Table 5. Selected Structural Parameters for 4 and 7[a]

	4	7		4	7
		Bond Lengths			
Fe–C1	2.040(6)	1.955(4)	C1–H1	0.99(6)	
Fe–C2	2.866(6)		C2–C0		1.478(6)
Fe–C3	1.762(7)	1.767(5)	C3–O3	1.141(7)	1.139(5)
Fe–C4	1.734(8)	1.759(5)	C4–O4	1.162(8)	1.140(5)
Fe–(C10–14)	2.115	2.118	C–C (Cp*)	1.417	1.418
Mn–C1		2.281(4)	C–Me (Cp*)	1.50	1.494
Mn–C2	1.837(6)	2.144(4)	C5–O5	1.150(8)	1.154(5)
Mn–C5	1.780(8)	1.770(5)	C6–O6	1.154(8)	1.160(5)
Mn–C6	1.763(8)	1.751(5)	C–C (Cp')	1.39	1.39
Mn–(C20–24)	2.150	2.153	C20–C25	1.50(1)	1.467(9)
C1–C2	1.269(8)	1.223(5)			
		Bond Angles			
Fe–C1–C2	118.1(5)	156.9(4)	C–C–Me (Cp*)	125.9	125.9
Mn–C1–C2		67.8(3)	C1–Mn–C6		83.8(2)
C2–C1–H1	127(4)		C1–Mn–C7		103.4(2)
Mn–C2–C1	178.7(5)	80.3(3)	C2–Mn–C5	91.8(3)	108.1(2)
C1–C2–C0		155.1(4)	C2–Mn–C6	90.4(3)	83.5(2)
C1–Fe–C3	88.5(3)	95.2(2)	C5–Mn–C6	88.1(3)	88.8(2)
C1–Fe–C4	95.1(3)	87.8(2)	Mn–C5–O5	179.3(6)	176.2(4)
C3–Fe–C4	94.9(3)	96.2(2)	Mn–C6–O6	177.9(6)	178.9(4)
Fe–C3–O3	176.6 (6)	177.9(4)	C–C–C (Cp')	108.0	108.0
C–C–C (Cp*)	108.0	108.0	C–C20–C25	125.7	126.6

[a] Bond lengths in Å and bond angles in deg. Values without standard deviations are averaged ones. For the bridging part see also Table 6 and Figure 2.

detected at all (eq 4). Characterization of **7** is based on (1)

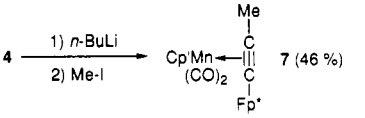

(4)

disappearance of the vinylidene C_α resonance at very low field and (2) the δ_C's for the acetylenic carbons (C1 and C2) which are comparable to those of Mn η^2-alkyne complexes (see, for example, **10**[20a] in Table 4). In the structure determined by X-ray crystallography (Figure 3

(20) (a) Lowe, C.; Hund, H.-U.; Berke, H. *J. Organomet. Chem.* **1989**, *378*, 211–225. (b) Cash, G. G.; Pettersen, R. C. *J. Chem. Soc., Dalton Trans.* **1979**, 1630–1633.

Table 6. Comparison of Structural Parameters of 4 and 7 with Related Compounds[a]

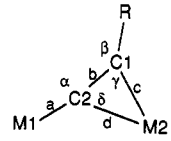

entry no.	complex	*a*	*b*	*c*	*d*	α	β	γ	δ	*d* − *c*	α − β	γ − δ
1	**10**[20a]	1.484(3)	1.227(3)	2.101(3)	2.103(2)	149.8(3)	154.4(3)	73.1(2)	73.0(2)	0.002	4.6	0.1
2	**11**[25]	1.47(1)	1.19(1)	2.114(6)	2.165(7)	157.7(7)	158.4(8)	76.1	71.5	0.051	0.7	4.6
3	**13**[4a]	2.19(2)	1.30(3)	2.10(2)	2.21(2)	146(2)	148(2)	77	68	0.11	2	9
4	**7**[b]	1.955(4)	1.223(5)	2.144(4)	2.281(4)	156.9(4)	155.1(4)	80.3(3)	67.8(3)	0.137	1.8	12.5
5	**2**[6a]	1.944(6)	1.244(9)	2.134(6)	2.357(5)	158.2(5)	147.2(6)	84.1(4)	64.2(3)	0.223	11	19.9
6	**1**[6a]	1.912(4)	1.226(6)	2.114(4)	2.422(5)	160.0(5)	152(4)	88.9(4)	60.8(4)	0.308	8	28.1
7	**12**[4b]	1.96(1)	1.25(2)	2.05(1)	2.53(1)	164(1)	*c*	97.3(8)	53.4(7)	0.48	*c*	43.9
8	**5**[18]	1.79(2)	1.33(2)	1.47(2)		176(2)	121(1)	121(1)			55	
9	**4**[b]	1.837(6)	1.269(8)	2.040(6)	2.866(6)	178.7(5)	127(4)	118.2(5)	38.9(4)	0.826	52.7	79.2

[a] Distances in Å: *a* = M1–C2, *b* = C2–C1, *c* = M2–C1, *d* = M2–C2. Angles in deg: α = ∠M1–C2–C1, β = ∠C2–C1–R, γ = ∠C2–C1–M2, δ = ∠C1–C2–M2. For the structures of the complexes, see text and Chart 2. [b] This work. [c] The position of R(H) was located artificially.

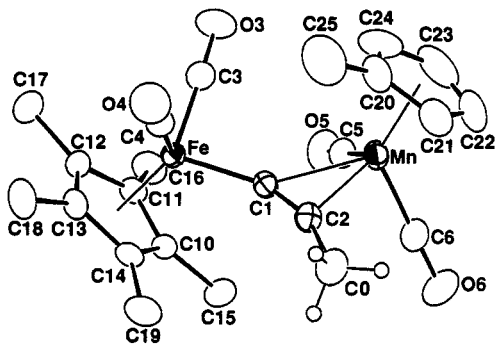

Figure 3. ORTEP view of **7** drawn at the 30% probability level.

and Table 5), the similar Mn—C1 and Mn—C2 distances (Figure 2) indicate clearly the dominant contribution of **A**.

Protonation of 4 and Reactivity of the Resulting Cationic Species. It is well-known that electrophilic addition to neutral η^1-vinylidene complexes occurs readily at the β-carbon to give η^1-alkylidyne complexes (eq 5).[8]

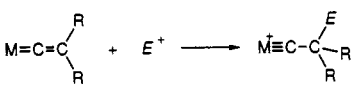

(5)

Reaction of **4** with HBF_4·OEt_2 in CH_2Cl_2 also proceeded smoothly to give red-violet **8**-BF_4 formulated as a heterobimetallic μ-vinylidene complex (eq 6). **4** was protonated

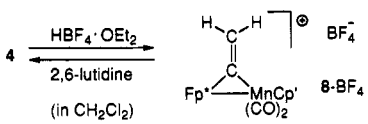

(6)

also by CF_3SO_3H and CF_3COOH (not by CH_3COOH) in CH_2Cl_2. However, in a basic solvent such as ether or THF, **4** remained unaffected by CF_3COOH, as judged by IR. In accord with this result, **8**-BF_4 was deprotonated by 2,6-lutidine to regenerate **4** in a quantitative yield (eq 6), while attempted deprotonation with a less bulky, more basic amine (NEt_3) resulted in the formation of an unknown adduct.

Treatment of **8**-BF_4 with a hydridic reagent (NEt_4BH_4) or successive treatment of **4** with HBF_4·OEt_2 and NEt_4BH_4 gave a mixture of products, from which was isolated a vinyliron complex **9** (eq 7). Although formation of a small

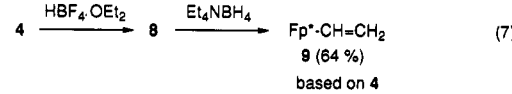

(7)

amount of a μ-vinyl complex was indicated by the characteristic deshielded signal (δ 10.23, dd, J = 7.7 and 11.0 Hz) of the reaction mixture, no Mn-containing product other than $Cp'Mn(CO)_3$ was isolated.

Some D-labeling experiments were conducted with respect to the transformation of **4** to **9**. Treatment of **4** with an excess amount of CF_3COOD followed by hydridic reduction gave **9**-d_2 whose methylene part was completely deuterated (eq 8). On the other hand, successive treatment

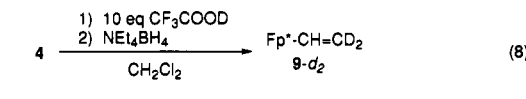

(8)

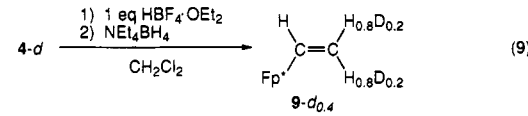

(9)

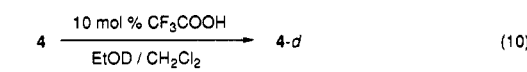

(10)

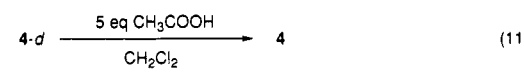

(11)

of **4**-*d* with HBF_4·OEt_2 (1 equiv) and NEt_4BH_4 afforded **9**-$d_{0.4}$ (eq 9). Although the amount of HBF_4·OEt_2 was adjusted carefully, a considerable part of the deuterium was lost probably owing to exchange with protic impurity in the reaction mixture. D was found equally in both the *cis* and *trans* sites within error of ^1H NMR analysis, and the apparent nonstereospecificity did not result from the protonation step of **4** but from the subsequent fast H–D exchange equilibrium. In fact, when **4** was stirred with EtOD in the presence of a catalytic amount of CF_3COOH, the vinylidene proton was completely deuterated (eq 10). Moreover, whereas **8**$^+$ was not obtained by treatment of **4** with acetic acid, C_2D in **4**-*d* exchanged readily with externally added CH_3COOH (eq 11).

4 did not react with bulkier electrophiles such as $MeOSO_2CF_3$, $Et_3O^+BF_4^-$, and $[Fp^+(THF)]BF_4^-$, probably owing to a steric effect of the Cp* ligand. Prolonged

Scheme 2

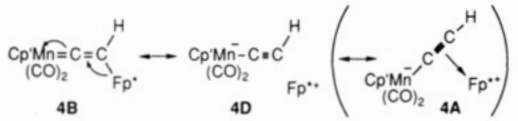

reaction with $Et_3O^+BF_4^-$ gave a small amount of **8**-BF_4 arising from an acidic impurity.

Discussion

Structure and Reactivities of Cp'Mn(CO)$_2$[=C=C(H)Fp*] (4). (i) Structure. The spectroscopic and crystallographic analyses of **4** reveal the dominant contribution of **4B** (Scheme 2). The structural deviations from normal η^1-vinylidene Mn complexes (points i and ii, vide supra) may be explained in terms of additional contribution of either the zwitterionic structure **4D** or the η^2 structure **4A**. The long Fe—C2 distance (*d*) may be consisent with the former structure, and the latter is implicated by the isoelectronic resonance structure (**1A**) of [Fp*$_2$(μ-C≡CH)]BF_4.[6a]

In order to evaluate the contribution of these two resonances structures, EHMO calculations on CpMn(CO)$_2$[=C$_\alpha$=C$_\beta$(H)Fp][1] (the Cp$_2$ analogue of **4**) and CpMn(CO)$_2$[=C$_\alpha$=C$_\beta$(H)Me] have been carried out and two results are derived. (1) In the Fp derivative, no attractive interaction between Fe and C$_\alpha$ is found and, therefore, the contribution of **4A** is negligible. (2) The substitution of the methyl group with Fp causes a decrease in the Mn—C$_\alpha$ overlap population and, at the same time, an increase in the C$_\alpha$—C$_\beta$ overlap population. In Figure 4 are shown the second HOMOs lying on the *xz* plane, which are significantly perturbed by the replacement of the vinylidene substituent. According to Hoffmann's calculation,[10] these orbitals originate from interaction of the filled a″-type Mn orbital with the empty $\pi^*_\parallel$-type C=C(H)R orbital and are responsible for back-donation. Because the energy level of the C=C(H)Fp π^* orbital is higher than that of the C=C(H)Me π^* orbital, back-donation to the former becomes less effective. As a result, the Mn—C$_\alpha$ distance in **4** is not as shortened as that in **5** (point i). In addition, it should be noted that, in the second HOMOs, the phase of the p$_x$ orbitals of the C$_2$H bridge is an antibonding combination, though weak. Therefore, as the extent of the back-donation decreases, the C$_\alpha$—C$_\beta$ interaction bears less antibonding character; in other words, the C$_\alpha$—C$_\beta$ bond order in CpMn(CO)$_2$[=C=C(H)Fp] increases (point ii). The situation described here is best characterized by the additional contribution of the zwitterionic resonance structure **4D**. Thus, **4D** and the structural changes i and ii are brought about by the donation from the Fp orbitals lying high in energy and being diffused compared to organic fragments such as CH_3. As a result, donation from the two metal centers makes the C$_2$H bridge highly nucleophilic.

(ii) Deprotonation of 4 and Subsequent Electrophilic Addition to the Resulting Anionic Ethynediyl Species Li[Cp'Mn(CO)$_2$C$_2$Fp*] (6). Treatment of **4** with *n*-BuLi does not result in nucleophilic attack at C$_\alpha$ but deprotonation of C$_2$*H* to generate the anionic ethynediyl species **6** (path *a* in Scheme 3). This is presumably due to the increased electron density at C$_\alpha$ caused by the donation from Fp* to the C$_2$H bridge as discussed above.

Although deprotonation of *cationic* η^1-vinylidene complexes giving neutral acetylide complexes has a number

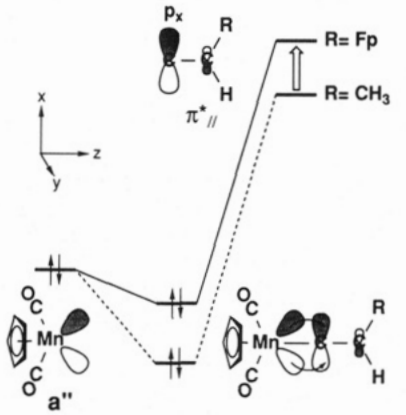

Figure 4. MO diagram for the [CpMn(CO)$_2$]–[=C=C(H)-Fp] interaction.

Scheme 3

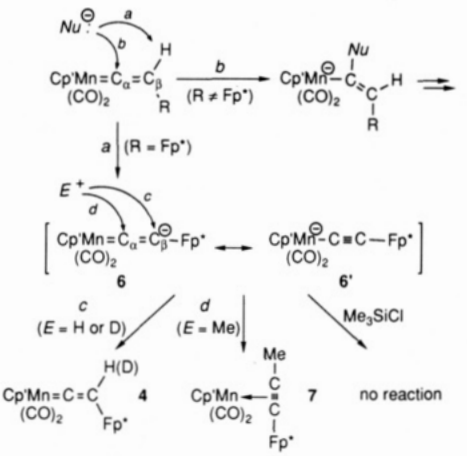

of precedents (eq 12),[8] few reports on the corresponding

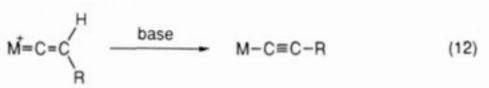

(12)

reaction of a *neutral* complex have appeared and nucleophilic reactions usually occur at C$_\alpha$[3a,8] (path *b* in Scheme 3). Geoffroy recently reported formation of the similar anionic Mn acetylide species [Cp'Mn(CO)(PPh$_3$)(C≡CR)]$^-$ via deprotonation of the *neutral* vinylidene complex Cp'Mn(CO)(PPh$_3$)[=C=C(H)R].[21] The unusual deprotonation was ascribed to PPh$_3$, because the CO analogue followed nucleophilic addition to C$_\alpha$. The anionic acetylide species is so nucleophilic as to react readily with various nucleophiles to give η^1-vinylidene complexes via addition to C$_\beta$.

The resonance structures of the anionic species **6** and **6'**, in which C$_\beta$ and Mn are preferred reaction sites, can explain the regiochemistry of the protonation but not that of the methylation (at C$_\alpha$). EHMO calculation of the Cp$_2$ analogue[14] supports the conventional electronic consideration (**6** ↔ **6'**). The CpMn(CO)$_2$'s MOs lying higher than the Fp's MOs makes the p coefficient of C$_\beta$ in the HOMO larger than that of C$_\alpha$, and in addition, C$_\beta$ is slightly more negatively charged than C$_\alpha$. Therefore, we now assume steric effects of the ancillary ligands to be a possible

(21) (a) Lugan, N.; Kelley, C.; Terry, M. R.; Geoffroy, G. L.; Rheingold, A. L. *J. Am. Chem. Soc.* **1989**, *111*, 7653–7654. (b) Kelley, C.; Lugan, N.; Terry, M. R.; Geoffroy, G. L.; Haggerty, B. S.; Rheingold, A. L. *J. Am. Chem. Soc.* **1992**, *114*, 6735–6749. (c) The anionic acetylides themselves are rare.[21b]

Scheme 4

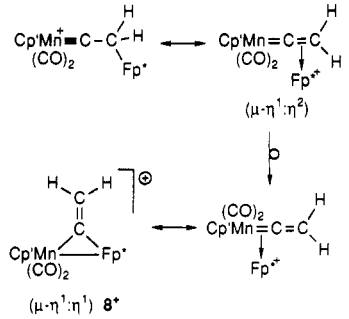

Scheme 5

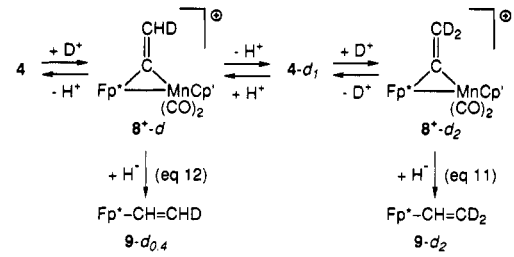

origin of the methylation at C_α; that is, a small electrophile such as H^+ attacks the more negatively charged C_β with the larger HOMO coefficient (path *c*; Scheme 3), whereas the bulky Cp* ligand prevents a sterically demanding electrophile from approaching C_β and, consequently, MeI attacks C_α to give **7** (path *d*).[22] In accord with this consideration, no reaction took place between **6** and Me_3SiCl, a more bulky electrophile.

(iii) Protonation of 4 Giving the Heterobimetallic μ-vinylidene Complex [(Cp'Mn)(Cp*Fe)(CO)₄(μ-C=CH₂)]⁺ (8⁺) and Subsequent Hydridic Reduction: Formal Hydrogenation of 3 to Fp*CH=CH₂ (9). As anticipated from the above EHMO analysis, **4** is basic enough to be protonated by $HBF_4{\cdot}OEt_2$, CF_3SO_3H, and CF_3COOH. For the resulting 8^+, two structures are possible as shown in Scheme 4. A reaction similar to eq 5 gives a bridging alkylidyne complex.[8] Transfer of d electrons of the Fe atom to C≡Mn gives rise to a μ-η^1:η^2-ethenylidene complex. Subsequent slippage of the vinylidene moiety (Mn=C=CH_2) on the Fp*⁺ center may form a μ-η^1:η^1-ethenylidene (so-called μ-vinylidene) complex. Although the quaternary carbon signal at low field (δ 280.1) may be consistent with all these structures, **8**-BF_4 can be characterized on the basis of the NMR data of the CH_2 moiety (δ_H 6.78, 7.15 (d × 2, J_{gem} = 11.5 Hz), δ_C 132.1 (t, J_{C-H} = 160 Hz)). First, the alkylidyne structure is eliminated by the nonequivalent CH_2 signals and the sp^2-(CH_2) character indicated by the J_{C-H} value. Second, both $\delta_{H,C}(CH_2)$'s of a μ-η^1:η^2-type complex appear at higher field than those of a μ-η^1:η^1-type complex whose noncoordinated CH_2 part ($\delta_{C,H}$) resonates in the normal olefin region (cf. $Cp^*_2Mo_2(\mu\text{-}\eta^1\text{:}\eta^2\text{-}C{=}CH_2)(CO)_4$,[23a] δ_H 2.37, 2.84 (d × 2, J_{gem} = 14 Hz), δ_C 45.3, 337.3; $Cp_2Mo_2(\mu\text{-}\eta^1\text{:}\eta^2\text{-}C{=}CMe_2)(CO)_4$,[23b] δ_C 79.8, 342.9; $Cp'_2Mn_2(\mu\text{-}\eta^1\text{:}\eta^1\text{-}C{=}CH_2)(CO)_4$,[24] δ_H 6.77 (s), δ_C 289.2 ($\delta(CH_2)$ not reported); $Cp^*_2Fe_2(\mu\text{-}\eta^1\text{:}\eta^1\text{-}C{=}CH_2)(\mu\text{-}CO)(CO)_2$,[6c] δ_H 6.63 (s), δ_C 113.4 (t, J_{CH} = 156.1 Hz), 295.5 (s)). Indeed, the NMR parameters of **8**-BF_4 are consistent with the μ-η^1:η^1 structure (a cationic heterobimetallic μ-vinylidene complex). In accord with this structure, the red-violet color indicates the presence of an Fe–Mn bond and no bridging CO has been detected by IR or ^{13}C NMR.

Subsequent hydridic reduction of 8^+ produces the vinyl complex **9** via a heterobimetallic μ-vinyl complex, presumably Cp'Mn(CO)Cp*Fe(CO)[μ-η^1(*Fe*):η^2(*Mn*)-CH=CH_2](μ-CO). The results of the labeling experiments (eqs 8–11), which are explained by the fast protonation-deprotonation equilibrium of **4** (Scheme 5), reveal the following mechanistic details. (1) The methylene protons in **9** come from the original C_2H and acid, and hydride is introduced as the methine proton. (2) On protonation of **4**, the Fe atom slips to C_α as assumed in Scheme 4. (3) Not only the protonation but also the Fe slippage (Scheme 4) is reversible. (4) On hydride addition to 8^+, H^- attacks C_α to give a μ-vinyl intermediate, from which the Mn moiety dissociates to release **9**. No μ-ethylidyne complex resulting from a C_β attack is detected at all by ^{13}C NMR of the reaction mixture.

Thus, Fp*C≡CH (**3**) is formally hydrogenated to Fp*CH=CH_2 (**9**) by way of the successive protonation–hydridic reduction ($H^+ + H^- = H_2$) of the C=C(H)Fp* ligand in **4**. It should be pointed out that during the formal hydrogenation the $FeC_A{\equiv}C_BH$ linkage in **3** is inverted as a result of the 1,2-H shift and the Fe slippage: **9** ($FeC_BH{=}C_AHH$).

Comparison of the Molecular Structure of 4 and 7 with Related Compounds: Change from the η² Structure (A) to the η¹-Vinylidene Structure (B) Relevant to the 1-Alkyne-to-Vinylidene Rearrangement. (i) Comparison of 4 and 7 with Related Compounds. Interestingly, although the three dinuclear complexes [(η^5-C_5R_5)M(CO)$_2$]$_2$(μ-C_2R) (**1**, **4**, and **7**) derived from **3** contain μ-C_2R as a unique bridging ligand and isoelectronic 16e (η^5-C_5R_5)M(CO)$_2$ (M = Fe^+, Mn) as metal components, their structures change from the η^2 structure (**7A**) to the η^1-vinylidene structure (**4B**) depending on the combination of the metal components (Figure 2).

In order to consider the electronic origin of the structural change, the ^{13}C NMR and structural parameters are compared with those of related compounds (η^1-vinylidene Mn complex **5**;[18] η^2-alkyne complexes **10**[20a] (Mn) and **11**[25] (Fe); related dinuclear μ-C_2R complexes **1**,[6a] **2**,[6a] **12**,[4a] **13**[4b]) (Tables 4 and 6, Chart 2, and Figure 2). Of the structural parameters listed in Table 6, $d - c$, $|\alpha - \beta|$, and $\gamma - \delta$ are equal to zero for an ideal η^2-alkyne complex (**A**) with the M2—C1—C2 isosceles triangle structure. As **B** contributes more, α and γ in addition to the above three parameters increase and β and δ decrease. As shown in Table 6, the complexes can be arranged to be consistent with the structural continuum **A**–**B** and, in particular, the monotonically changing γ, $d - c$, $\gamma - \delta$ (increasing), and δ

(22) **4**-*d* and **7** may be formed via the initial reaction at Mn giving $Cp'Mn^{IV}(CO)_2(E)(C{\equiv}CFp^*)$ (E = H (D), Me) followed by reductive elimination producing $Cp'Mn(CO)_2(\eta^2\text{-}EC{\equiv}CFp^*)$. When E = H, a 1,2-H shift would give **4**. Although we have no evidence to eliminate this reaction pathway, to our knowledge (η^5-C_5R_5)$Mn^{IV}(CO)_2(R_1)(R_2)$, where either R_1 or R_2 is hydrocarbyl, has not been reported so far[17] and most electrophilic additions to anionic acetylide species except for some basic Ir complexes give η^1-vinylidene complexes through reaction at the β-carbon.[8,21] Another possible mechanism involves the exclusive reaction at C_α giving $Cp'Mn(CO)_2(\eta^2\text{-}EC{\equiv}CFp^*)$. This mechanism is unlikely, judging from the present EHMO analysis.

(23) (a) Doherty, N. M.; Elschenbroich, C.; Kneuper, H.-J.; Knox, S. A. R. *J. Chem. Soc., Chem. Commun.* **1985**, 170–171. (b) Froom, S. F. T.; Green, M.; Mercer, R. J.; Nagle, K. R.; Orpen, A. G.; Rodrigues, R. A. *J. Chem. Soc., Dalton Trans.* **1991**, 3171–3183.

(24) Alt, H.; Engelhardt, H. E.; Steinlein, E.; Rogers, R. D. *J. Organomet. Chem.* **1987**, *344*, 321–341.

(25) Reger, D. L.; Klaeren, S. A.; Lebioda, L. *Organometallics* **1988**, *7*, 189.

Chart 2

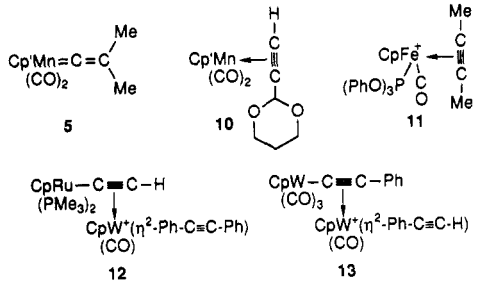

(decreasing) prove to be good indicators. A similar tendency is evident for the ^{13}C NMR data [see δ(C2) − δ(C1), Table 4).

Thus, it turns out that the structure of **7** lies within the structural continuum **A**–**B** and is much closer to **A** than is the case for the isoelectronic **1** and **2**. On the other hand, the structure of **4** is outside **A**–**B** and the contribution of **D** is evident, as indicated by the above-mentioned EHMO analysis.

When it is assumed that the dinuclear bridging alkynyl complex XY(μ-C_2R) consists of an interaction between the alkynyl part XC≡CR and the metal fragment Y, the structure of XY(μ-C_2R) containing first-row transition-metal components[26] depends on a balance of the forward donations and back-donations (Scheme 6), in other words, balance of the electron-donating abilities of X and Y. In Scheme 7 the structures and selected EHMO parameters are arranged according to the schematic representation of the structural continuum **A**–**B**. (The charges of X, Y, and R are adjusted to be consistent with **A**.) In the middle rows, the parameters for the π(C_α—C_β) orbital (HOMO: **E**, **E**′) of XC≡CH are listed. (XC≡CH is the simplified model compound of XC≡CR where *Fe*, *Mn*, and R are fixed to $CpFe(CO)_2$, $CpMn(CO)_2$, and H, respectively. Linear structures are assumed.) E_d is its energy level, and p_α and p_β are the *p* coefficients of C_α and C_β, respectively. This orbital interacts with M2(Y)'s empty σ-type orbital as shown in **F** (Scheme 7). At the bottom of the table, the energy levels (E_{bd}) of Y's a″-type orbital which back-donates to the XC≡CH ligand (see **H** and **H**′) are listed.

At first sight, as X becomes more electron-donating (CH_3 → Fe → Mn; compare the E_d values), the structure tends to shift from **A** to **B**. Furthermore, the structures of XY(μ-C_2R) can be rationalized according to the following three situations. (1) In the case of **10** and **11** where X (organic groups) does not significantly perturb the symmetrical structures and the lower-lying energy levels of the HOMO and LUMO of XC≡CH, an **A**-type structure results from the typical Dewar–Chatt–Duncanson interaction (**F** + **H**; $E_{bd} > E_d$). (2) When X is a metal component, π-electron donation to the C_2H moiety makes the p_α orbital larger than the p_β orbital (**E**′: see p_β/p_α in Scheme 7). Then M2 slips to the direction of C_β in order to maximize the overlap with the larger p_β orbital (**F**′). As to the back-donation (**H**′), when X (M1) is a strong π donor such as *Mn*, the metal-based **G**′ orbital with less C_2H character is pushed up higher in energy. Then the interaction **H**′ becomes less important and, as a whole, a **B**-type structure results from the dominant contribution of **F**′ irrespective of the electron-donating ability of Y, as typically exemplified by **4** and **5**. (3) The complexes **7**, **2**, and **1** (X = *Fe*), where **G**′ has substantial *p* coefficients and E_d is comparable to E_{bd}, are intermediate between these two extremes. A strongly π-electron-donating M2(Y) may interact sufficiently with **G**′ to stabilize an **A**-type structure. In fact, **7** bearing more electron-donating *Mn* (M2) is closer to **A** than the isoelectronic **1** and **2** bearing *Fe* (M2).

Thus, as X becomes more π electron donating and, at the same time, Y becomes less so, forward donation (**F**′) emerges from behind back-donation (**H**) which binds Y closer to C_α and, consequently, the structure changes from **A** to **B**, as typically displayed in Figure 2.

(ii) Relevance to the 1-Alkyne-to-Vinylidene Rearrangement. The positions of M1, M2, and R of the complexes listed in Table 6 are plotted with respect to the C≡C bridge (Figure 5). We can see the situation that, as X becomes more electron-donating (or the entry number increases), the X—C_α—C_β part becomes linear and the angle $\angle C_\alpha$—C_β—Y approaches 120°.[27]

The movement of the three substituents (X, Y, and R) around the C_α—C_β moiety as one goes from **A** to **B** reminds us of the intramolecular 1,2-H shift mechanism of the 1-alkyne-to-vinylidene rearrangement proposed by Hoffmann et al.[10] (eq 1 and Scheme 8). The 1,2-H shift is initiated by rotation of M, H, and R around the C≡C part (or slippage of M). In the following symmetrical transition state, the H atom is delivered from C_α to C_β. As the system rotates further, C_β's orbital becomes larger, finally to form a σ bond with H and produce an η^1-vinylidene complex. The structural change of the XY(μ-C_2R) complexes shown in Figure 5 corresponds to the latter half (after the transition state) of this process. The most significant difference between these two systems is that the 1,2-H shift (Y = H) lacks the **H**′-type stabilization which keeps Y closer to C_α, although the **F**(**F**′)-type interaction is available for both systems. Therefore, in the case of the 1,2-H shift, after the transition state the H atom (Y) slips to C_β so spontaneously as to accomplish the ligand transformation. However, in the case of the dinuclear complexes intermediate structures are stabilized by balancing the two interactions **F**′ and **H**′, i.e. a scramble for C_α's empty p orbital by the two filled metal orbitals with appropriate symmetry. As M1—C_α—C_β stretches (the 1,2-H shift; Scheme 8) or as the π-electron-donating ability of M1 increases (the dinuclear complexes), the d_π(M1)–p_π(C_α) back-donation (**F**′) stabilizing **B** becomes more effective and instead the d_π(M2)–p_π(C_α—C_β) back-donation (**H**′) stabilizing **A** becomes less important. These results mainly originate from the fact that a strongly π-electron-donating metal (M1) tends to stabilize **B** rather than **A**, as already pointed out by Hoffmann et al.[10] It should be noted that, as one moves from **A** to **B**, the C_α and C_β coefficients monotonically change in a manner similar to those of the orbitals depicted in Scheme 8. (Both p_β/p_α (the dinuclear complexes) and C_β orbital/C_α orbital (the 1,2-H shift) increase.) Thus, the XY(μ-C_2R) systems

(26) The situations for **12** and **13**, containing the second- and/or third-row metals and the 4e-donating η^2-alkyne ligand, are somewhat dissimilar from the present Fe, Mn system. Because the Ru and W orbitals lie too far above the C_2H orbitals to mix with each other, **E**′ is not as influenced by M1 (=Ru, W) as in the case of M1 being the first-row metals; i.e., **E**′ (M1 = Ru, W) resembles **E** with respect to its energy level as well as the symmetrical structure. In addition, the energy level of the filled a″-type W orbital is comparable to that of **G**. Consequently, the **A**-type structure results from the strong back-donation (**H**). The deformation of **12** toward **B** should originate from the steric repulsion due to the bulky PMe_3 ligands on the Ru center.

(27) Although $\angle C_\alpha$–C_β–R also approaches 120°, the relationship with the electron-donating ability of X is not as straightforward as that of $\angle$X–C_α–C_β and $\angle C_\alpha$–C_β–Y. This is partly due to the fact that some of the complexes contain H atoms whose positions are not well-defined by X-ray crystallography.

Scheme 6

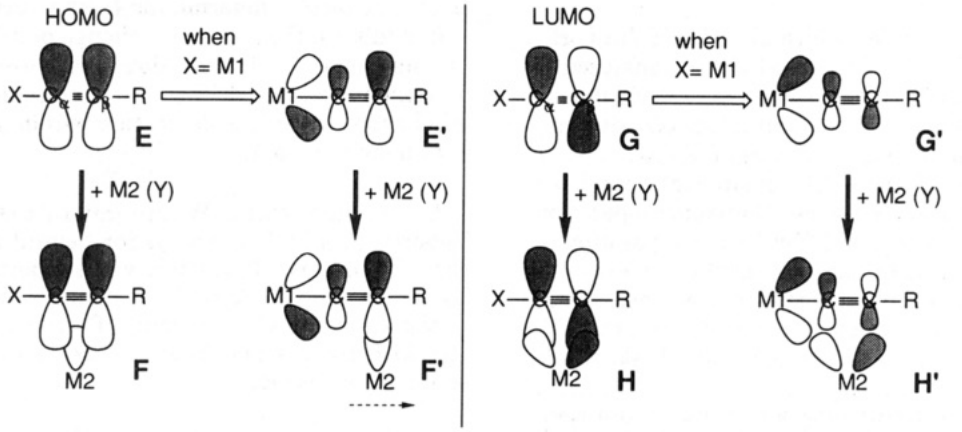

Scheme 7

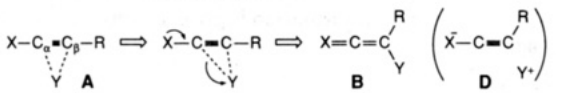

Complex [a]	12	13	7	2	1	5	4
X	[b]	CH_3	*Fe*	*Fe*	*Fe*	*Mn*⁻	*Mn*⁻
Y	*Mn*	*Fe*⁺	*Mn*	*Fe*⁺	*Fe*⁺	CH_3^+	*Fe*⁺
R	H	CH_3	CH_3	Ph	H	CH_3	CH_3
E_σ [c]	-13.6	-13.6	-12.2	-12.2		-11.4	-11.4
p_α	0.61	0.61	0.14	0.14		0.03	0.03
p_β	0.61	0.61	0.38	0.38		0.31	0.31
p_β / p_α	1.0	1.0	2.7	2.7		10.3	10.3
E_{bd} [d]	-11.8	-12.4	-11.8	-12.4		—	-12.4

[a] *Fe* = $(\eta^5\text{-}C_5R_5)Fe(CO)(L)$; *Mn* = $(\eta^5\text{-}C_5R_5)Mn(CO)_2$. [b] $-\overline{CH[O(CH_2)_3O]}$. [c] Parameters for the HOMO of the model complex, XC≡CH (see text). [d] Energy levels for the a″-type orbitals of the Y fragment.

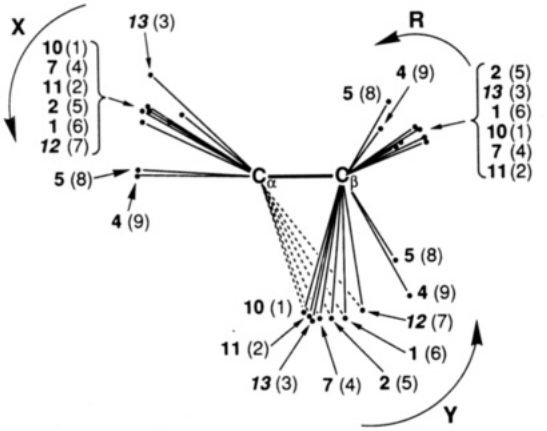

Figure 5. Plots of X, Y, and R of the dinuclear complexes. The C_α–C_β length is fixed at 1.22 Å, and it is assumed that X, Y, R, C_α, and C_β lie on the same plane. Numbers in parentheses are the entry numbers of Table 6. The italicized **12** and **13** contain second- and/or third-row metals as well as a 4e-donating η^2-alkyne ligand.[26]

can be viewed as structural models for intermediate states of the 1-alkyne-to-vinylidene rearrangement.

Conclusion

The introduction of Fp* as the substituent (R) in the Mn η^1-vinylidene complex $(\eta^5\text{-}C_5R_5)Mn(CO)_2[=C=C(H)R]$ brings about significant structural and electronic changes, as summarized below.

Scheme 8

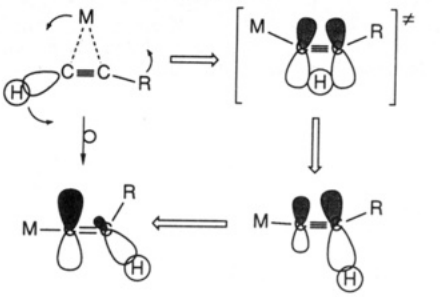

Scheme 9

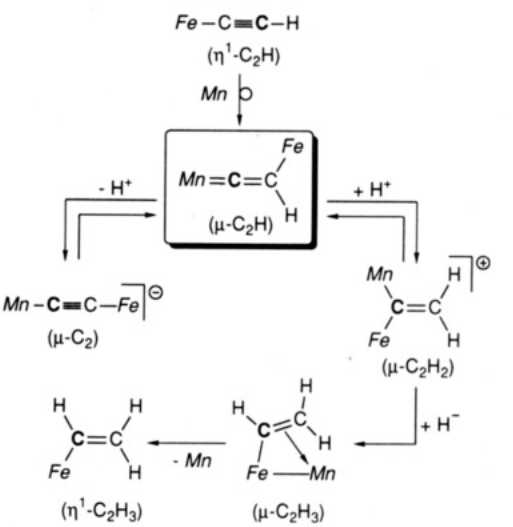

On coordination of **3** to a $Cp'Mn(CO)_2$ fragment, the heterobimetallic complex $Cp'Mn(CO)_2[=C=C(H)Fp^*]$ (**4**) forms via a 1,2-H shift in a manner similar to the reaction of 1-alkynes. **4** is characterized as an iron-substituted vinylidene complex (**B**) with the additional contribution of the zwitterionic structure **D**, in contrast to the isoelectronic **1** and **2**, which are analyzed as a resonance hybrid of **A** and **B**. The C_2H bridge in the resulting **4** serves as a carbon acid as well as a carbon base. Such amphoteric reactivity of **4** realizes the transformation of the η^1-C≡CH ligand in **3** into various elementary C_2 species such as μ-ethynediyl (–C≡C–; **6**), μ-ethenylidene (>C=CH_2; **8**), and η^1-ethenyl (–CH=CH_2; **9**) by way of deprotonation or sequential H addition of the μ-ethenylidenyl ligand (=C=C(H)–) in **4** (Scheme 9).[28] Furthermore, protonation of the vinyl ligand would lead to

η^1-ethylidene (=$CHCH_3$) and subsequently to η^2-ethylene (CH_2=CH_2) species.[29]

The structures of complexes formulated as $XY(\mu\text{-}C_2R)$, in particular, $[(\eta^5\text{-}C_5R_5)M(CO)_2]_2(\mu\text{-}C_2R)$, are analyzed as a resonance hybrid of the η^2 structure (**A**), the η^1-vinylidene structure (**B**), and the zwitterionic structure (**D**), depending on the electron-donating abilities of X (M1) and Y (M2). Although heterobimetallic complexes have been expected to exhibit a reactivity resulting from cooperation of the two metal centers, the difficulty in preparation of a series of isoelectronic (or isostructural) complexes has prevented us from examining the role of each metal component. The accumulated structural data for the $XY(\mu\text{-}C_2R)$-type complexes and their rather simple electronic structures have led us to the successful analysis of the electronic factors determining their structures.

In addition, the structural change of $XY(\mu\text{-}C_2R)$ as X becomes more π electron donating corresponds to the movement postulated for the intramolecular 1-alkyne-to-vinylidene ligand transformation within a metal coordination sphere (eq 1).

Acknowledgment. We are grateful to Prof. Kazuyuki Tatsumi (Osaka University) for helpful discussions on EHMO analysis. This study was supported partly by a grant from the Ministry of Education, Science, and Culture of the Japanese Government. Thanks are also due to Hideki Hirakawa and Satoshi Kakuta for their helpful technical assistance.

Supplementary Material Available: Tables of anisotropic thermal parameters and bond lengths and angles for 4 and 7 (10 pages). Ordering information is given on any current masthead page.

OM930614V

(28) For a similar ligand transformation on a diruthenium system, see: Colborn, R. E.; Davies, D. L.; Dyke, A. F.; Endesfelder, A.; Knox, S. A. R.; Orpen, A. G.; Plaas, D. *J. Chem. Soc., Dalton Trans.* **1983**, 2661–2668.

(29) (a) Casey, C. P.; Miles, W. H.; Tukada, H.; O'Conner, J. M. *J. Am. Chem. Soc.* **1982**, *104*, 3761–3762. (b) Kremer, K. A. M.; Kuo, G.-H.; O'Connor, E. J.; Helquist, P.; Kerber, P. C. *J. Am. Chem. Soc.* **1982**, *104*, 6119–6121. (c) Brookhart, M.; Studabaker, W. B. *Chem. Rev.* **1987**, *87*, 411–432.